

An application of Monte Carlo method to simulate disorders in polymer crystals

Takashi Yamamoto

Department of Physics, Faculty of Science, Yamaguchi University, Yamaguchi, Japan
(Received 1 July 1982)

The Monte Carlo method is applied to polymer crystals of idealized linear chain molecules of 30 carbon atoms, and the unharmonic, large-amplitude, oscillations and the subsequent conformational disorders of the chains are investigated. A crystalline field that confines the chain is treated by the molecular field approximation, and assumed to be cylindrical in this work. A production type simulation is adopted taking into account rigorous statistical weights for each sample conformation. Both the rotational isomeric model and the continuous rotation model of chain conformation are considered. By averaging over 10^4 – 8×10^4 chains, mean-square end-to-end distance, fractions of *gauche* and *trans* states and a detailed distribution of internal rotation angle are obtained. The effects of temperature and pressure on the conformation of the chain in the crystals are also simulated.

Keywords Monte Carlo method; conformational disorders; polymer crystals; crystalline field; high pressure

INTRODUCTION

In polymer crystals, molecular motions with large amplitude, and inevitably unharmonic, oscillation of internal rotation angles are known to be the origins of various phenomena, namely dielectric relaxation, crystalline phase transition, chain diffusion along its axis, etc. The chains in such large-amplitude motions are in a state of conformational disorder.

The geometry and the energetics of the conformational disorder have been studied by many workers. These studies were always done on the basis of particular, and more or less arbitrary, models of conformational disorder. No strict statistical mechanical calculations without recourse to the particular model has been done. This is mainly because of the mathematical difficulties in incorporating the interchain interactions into the calculation.

Monte Carlo calculations have frequently been used in conformational problems in polymer solutions. In these calculations, either a single chain free from interchain interaction or a many-chain system with relatively weak interchain interactions was considered. The same procedure as that used in a many-chain system does not work well in the present case of polymeric crystals.

The purpose of the present paper is to show that the Monte Carlo method used in the single-chain problem can be applied successfully to simulate conformational disorders in crystals by simplifying the interchain interactions and by estimating a rigorous statistical weight for each sample chain.

The chains in the crystals are more or less straightened and laid parallel with each other. The interchain interaction can be treated, as a first approximation, by assuming that the chains are in cylindrical potential wells produced by neighbouring chains. This approximation is valid when we are concerned with a highly disordered system, such as the high-pressure phase of polyethylene to which we shall refer later in this paper or the high-

temperature phase of polytetrafluoroethylene, where reduction of interchain correlation due to the smearing effect of interchain interaction and the high symmetry of hexagonal packing of the chains allow the molecular field approximation with cylindrical potential to be used. Similar Monte Carlo calculations can be done for crystals of lower molecular packing symmetry, such as orthorhombic polyethylene crystal, only by modifying the interchain potential. The application of the Monte Carlo method to simulate the behaviour of a chain in the crystal is scarcely found in the literature. It will give us an exact solution of the non-linear problem of chain conformation without recourse to any particular model.

CALCULATION METHOD

Monte Carlo calculations used in the studies of the conformations of polymers in solution are divided into two types. One is a method used, for example, in the recent work by Curro¹, where a successive sample conformation of the chain is generated by changing one internal rotation angle at a time. This method is analogous to the original Monte Carlo calculation by Metropolis *et al.* first applied to physical problems. The other type is that used by Rosenbluth *et al.*² Each sample chain is generated by attaching one structural unit after another till whole chain is completed. According to the terminology used by Teramoto *et al.*³, this is called a simulation of 'production type'.

A difficulty in applying the former method to dense systems is easily recognized. Strong intermolecular interactions make most of the successively generated chain conformations high-energy ones, which contribute little to the results. The method we shall apply is the latter production type one. For brevity of discussion in this section, the method of computation is explained for the rotational isomeric model. Extension to the more general case of the continuous rotation model, which is treated in the last section of this paper, is easy and direct.

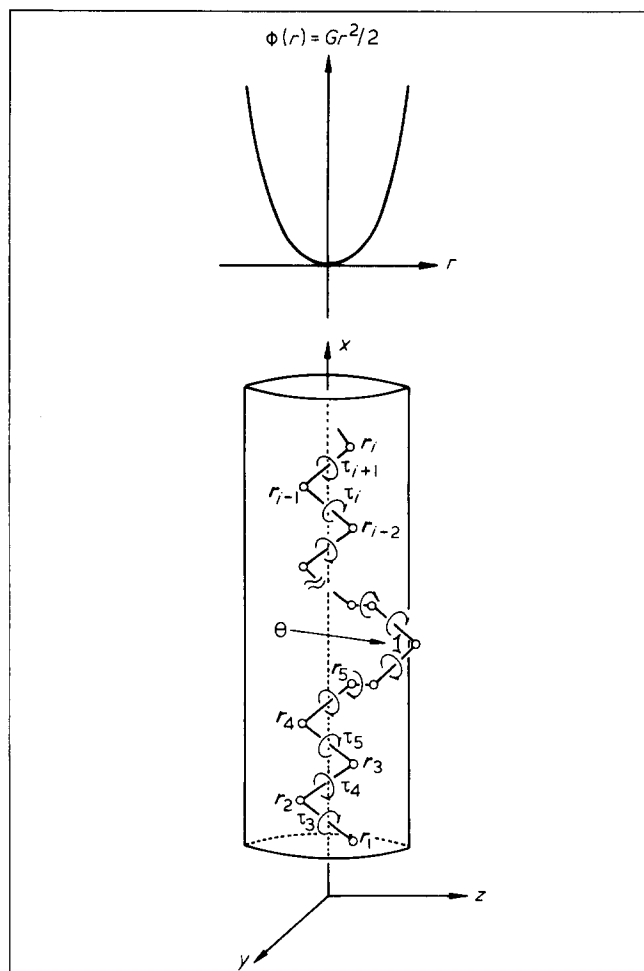


Figure 1 A molecular chain in cylindrical potential $\Phi(r)$. The positions of the first atom r_1 and the second atom r_2 are fixed as $r_1 = (0, 0, 0.445)$ and $r_2 = (1.25, 0, -0.445)$

Figure 1 shows a chain in a cylindrical potential. We construct the chain in the following way. We consider that the position of the first atom (r_1) and that of the second atom (r_2) are fixed. Then the position of the i th atom (r_i) is determined by $i-2$ internal rotation angles ($\tau_3, \tau_4, \dots, \tau_i$) through the usual transformation method. Assuming that the positions of $i-1$ atoms, and consequently $i-3$ internal rotation angles, are determined, we choose the value of the i th internal rotation angle τ_i from three possibilities, namely $\pm 120^\circ$ and 0° corresponding to three rotational isomeric states, with a probability $P_i(\tau_3, \tau_4, \dots, \tau_{i-1}/\tau_i)$:

$$P_i(\tau_3, \dots, \tau_{i-1}/\tau_i) = \exp(-\beta H_i) / Z_i(\tau_3, \dots, \tau_{i-1})$$

$$H_i = E(\tau_i) + E(G^+G^-) + E(\text{excl.}) + \Phi(r_i)$$

$$Z_i(\tau_3, \dots, \tau_{i-1}) = \sum_{\tau_i} \exp(-\beta H_i)$$

where $E(\tau_i)$ is the bond energy for internal rotation angle τ_i , $E(G^+G^-)$ and $E(\text{excl.})$ are extra energies due to bond sequence of opposite senses of *gauche* and to the excluded volume effect respectively, and $\Phi(r_i)$ is an intermolecular potential energy of i th atom. The probability P_i is normalized to unity for each i , and the normalization constant is expressed as Z_i .

By attaching one atom after another in this way, we can construct a whole chain, whose internal rotation angles are $\tau_3, \tau_4, \dots, \tau_N$, with probability $P(\tau_3, \tau_4, \dots, \tau_N)$:

$$\begin{aligned} P(\tau_3, \tau_4, \dots, \tau_N) &= \prod_{i=3}^N P_i(\tau_3, \dots, \tau_{i-1}/\tau_i) \\ &= \exp\left(-\beta \sum_{i=3}^N H_i\right) / \prod_{i=3}^N Z_i \\ &= \exp[-\beta H(v)] / Z(v) \quad v = (\tau_3, \tau_4, \dots, \tau_N) \end{aligned} \quad (1)$$

where $H = \sum H_i$ is the total Hamiltonian of the chain, Z is defined as $Z = \prod Z_i$, and β is the reciprocal of the thermal energy.

As seen in equation (1), the probability P does not correspond to a probability distribution at thermal equilibrium. A thermal average of any physical quantity A over a Boltzmann distribution is given as follows:

$$\begin{aligned} \langle A \rangle &= \frac{\sum_v A(v) \exp[-\beta H(v)]}{\sum_v \exp[-\beta H(v)]} \\ &= \frac{\sum_v P(v) Z(v) A(v)}{\sum_v P(v) Z(v)} \\ &= \frac{\langle AZ \rangle'}{\langle Z \rangle'} \end{aligned} \quad (2)$$

where $\langle \rangle'$ represents an average over the distribution $P(v)$ in equation (1). In this way a thermal average of any quantity $\langle A \rangle$ can be obtained from the average over all conformations $\langle \rangle'$ generated through equation (1).

The computation was done for the chain composed of 30 atoms ($N=30$), whose bond length r and bond angle θ were taken as $r=1.54$ and $\theta=109.47^\circ$ (the value for the diamond lattice). The extra energies $E(G^+G^-)$ and $E(\text{excl.})$ were assumed to be infinitely large, which means a complete rejection of the bond sequence G^+G^- and the chain overlap. The average $\langle \rangle'$ in equation (2) was obtained by the average over $10^4 - 8 \times 10^4$ chains according to whether the convergence was fast or slow.

In this study, the intermolecular potential $\Phi(r)$ is assumed to be quadratic: $\Phi(r) = Gr^2/2$. Similar calculation can be done for any arbitrary function $\Phi(r)$. The effect of varied functional form for $\Phi(r)$ on the conformation of the chain in the crystal is a subject of future studies.

RESULTS AND DISCUSSIONS

Rotational isomeric model

First we performed a calculation for the rotational isomeric model of chain conformation, where internal rotation angles $\{\tau\}$ are allowed to take values 0° to $\pm 120^\circ$ corresponding to *trans* and *gauche* states respectively. As shown later in this paper, the rotational isomeric model does not reproduce well a real conformation of the chain in the crystals, where internal rotation angles are considered to deviate seriously from those of the rotational isomeric model. This model, however, requires relatively short CPU time of computation, and therefore is available in obtaining the overall view of the behaviour of the chain. The energy difference between *trans* and *gauche* was

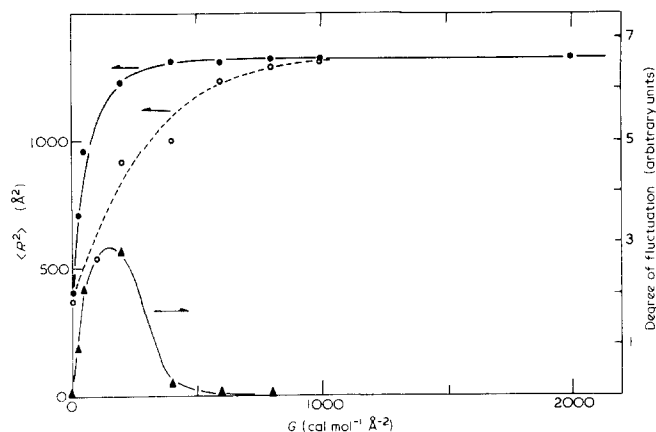


Figure 2 Mean-square end-to-end distances at 300 K (●) and at 500 K (○), and the degree of fluctuation of end-to-end distance at 300 K (▲) vs. G for the rotational isomeric model

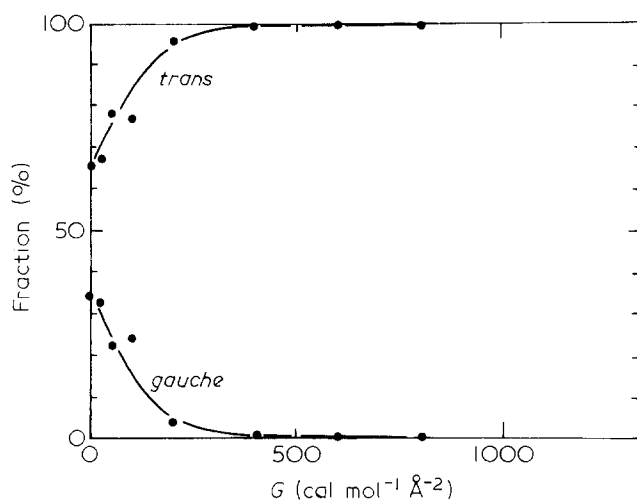


Figure 3 The fraction of *trans* and *gauche* bonds vs. G at 300 K for the rotational isomeric model

assumed to be 530 cal mol^{-1} : $E(0^\circ) = 0 \text{ cal mol}^{-1}$, and $E(\pm 120^\circ) = 530 \text{ cal mol}^{-1}$.

Figure 2 shows a change of the mean-square end-to-end distance $\langle R^2 \rangle$ with parameter G of interchain potential at 300K and 500K. The value of $\langle R^2 \rangle$ at 300K increases rapidly from about 400 \AA^2 for the coiled state at $G=0$ to 1330 \AA^2 for the extended state at $G \approx 500$. We note that the effective radius r_c of the cylindrical potential $\Phi(r) = Gr^2/2$ can be estimated from $Gr_c^2/2 = kT$. The value of $G=500$ means a cylindrical potential with effective radius $r_c = 1.5 \text{ \AA}$, which is of the order of one bond length.

A degree of thermal fluctuation of squared end-to-end distance R^2 , estimated from the statistical error of the average $\langle R^2 \rangle$ over 10^4 chains, is also plotted in Figure 2. The fluctuation has a sharp maximum around $G=150$, where the chain shows a rapid change from disordered coiled state to regular 2-1 helical state. This seems to correspond to an increase of fluctuation which is generally observed near the phase transition point.

Figure 3 shows the fraction of *trans* and *gauche* bonds vs. G . The fraction of *gauche* bonds decreases from about 35% at $G=0$ to about 0.3% at $G=800$. At $G=800$, $\langle R^2 \rangle$ is estimated to be 1323 \AA^2 , which means a contraction of fibre period of about 0.26%. The observed contraction of

fibre period for polyethylene is about 0.3% at 300K. The calculated conformation at $G=800$ at 300K is, therefore, considered to correspond to that of polyethylene molecule at 300K at atmospheric pressure, as far as the rotational isomeric model is concerned. The calculated value of 0.3% for the *gauche* fraction at 300K shows a presence of the order of one defect per stem.

As described before, the rotational isomeric model is not a correct picture of the chain conformation in the crystal, therefore for large G . The chain conformation for small G is, however, well represented by the rotational isomeric model as described later. Figure 4 shows the changes of $\langle R^2 \rangle$ with temperature for small values of G . At $G=0$, $\langle R^2 \rangle$ shows a steep descent at 100K from that of an ordered 2-1 helix to that of a disordered coil: the helix-coil transition. With the increase of G , the change of $\langle R^2 \rangle$ becomes gradual. A sigmoidal decrease of $\langle R^2 \rangle$, however, shows that the change of $\langle R^2 \rangle$ for large G can be regarded as a diffuse helix-coil transition of the chain in a cylindrical potential. A diffuse transition observed in PTFE around 150°C is considered to correspond to such a diffuse transition⁴.

Continuous rotation model

As described before, the rotational isomeric model suffers a serious disadvantage, in that the usual picture of molecular motion is lost in terms of oscillation of internal rotation angles. We now consider a continuous rotation model, in which the internal rotation angles take continuous values from -180° to $+180^\circ$, instead of discrete values of 0° and $\pm 120^\circ$ as in the rotational isomeric model. In carrying out the computation, however, we must limit the number of internal rotation angles within executable range. In the present study, 20 different internal rotation angles were considered:

$$\tau_i = -180^\circ + (360^\circ/20)(i-1) \quad (i=1-20)$$

Figure 5 shows the energy of internal rotation, $E(\tau)$, assumed in this study due to the first-order interaction. Similarly to the calculation for rotational isomeric model,

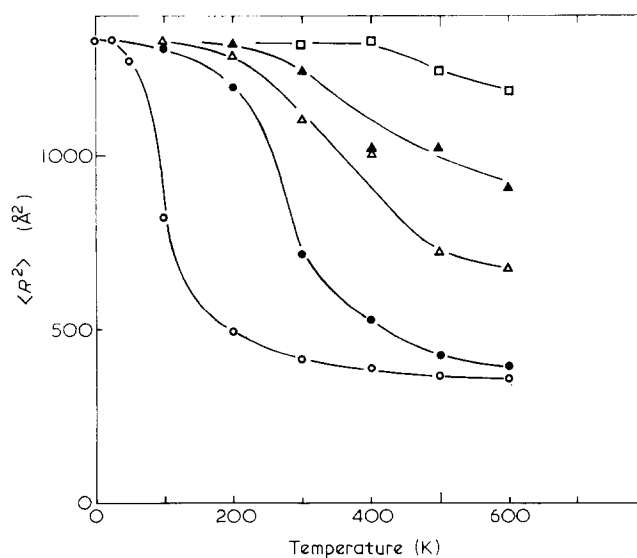


Figure 4 Changes of mean-square end-to-end distance $\langle R^2 \rangle$ with temperature for $G=0$ (○), $G=25$ (●), $G=100$ (△), $G=200$ (▲) and $G=600$ (□) for the rotational isomeric model

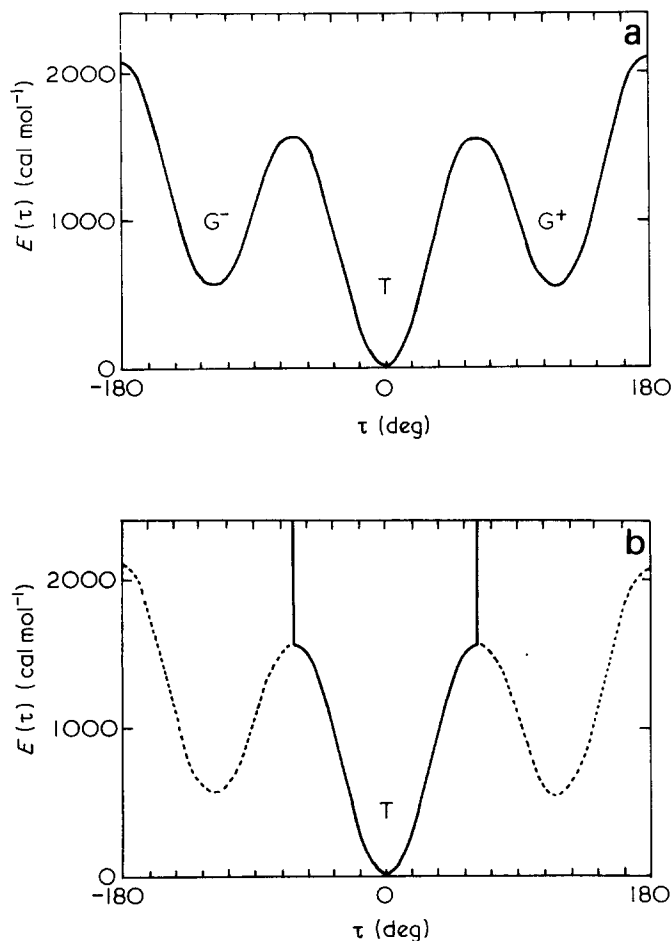


Figure 5 Energies of internal rotation $E(\tau)$ for the continuous rotation model (a), and for the restricted rotation model (b)

the second-order interaction which forbids a sequence of *gauche* bonds of opposite sense and the excluded volume effect were taken into account.

The change of $\langle R^2 \rangle$ with G at 300K and 550K are shown in Figure 6. The value of $\langle R^2 \rangle$ changes gradually with G , in contrast to the result for the rotational isomeric model.

A contraction of fibre period with increase of temperature has often been observed in polymer crystals. For example, the fibre period of polyethylene crystal decreases by about 0.1% per 100K rise. The phenomenon has been explained either by the thermal oscillation of the internal rotation angles around the *trans* state or by the excitation of conformational defects with large deviation of internal rotation angles from the *trans* state. In order to separate these two contributions, we examined the behaviour of $\langle R^2 \rangle$ of the chain with restricted potential of internal rotation (Figure 5b), which allows oscillation around the *trans* state only. The results for the chain, $\langle R^2 \rangle_{\text{restr}}$, at 300K and 550K are also shown in Figure 6. The difference between $\langle R^2 \rangle$ for the continuous rotation model and that for the restricted rotation model shows the contribution of bonds around the *gauche* state, which we hereafter call 'gauche bond' for brevity. At small G , the contraction of the chain is due mainly to the excitation of *gauche* bonds. The contribution of the *gauche* bonds decreases with increase of G and becomes almost zero at $G=5000$ for 300K for example. The data for $\langle R^2 \rangle$, $\langle R^2 \rangle_{\text{restr}}$ and $\langle C \rangle$ at 300K and 550K are listed in Table 1 and Table 2, where

$\langle C \rangle$ is the average fibre period. The observed contraction of fibre period of 0.3% for polyethylene crystal at room temperature shows a corresponding value of G of more than $5000 \text{ cal mol}^{-1} \text{ \AA}^{-2}$ in the continuous rotation model. The observed contraction of fibre period is, therefore, considered to come almost entirely from the oscillation around the *trans* state.

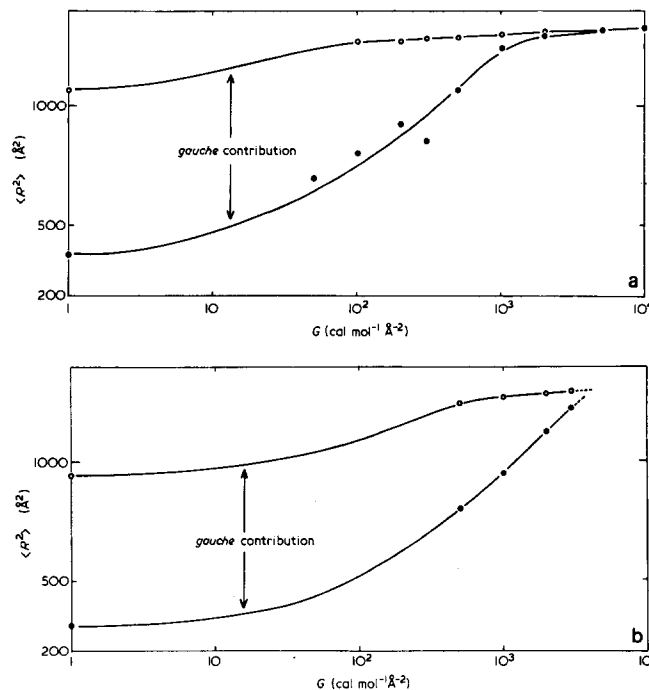


Figure 6 Changes of $\langle R^2 \rangle$ for the continuous rotation model (●) and $\langle R^2 \rangle_{\text{restr}}$ for the restricted rotation model (○) vs. G at (a) 300 K and at (b) 550 K

Table 1 The values of $\langle R^2 \rangle$, $\langle C \rangle$ and $\langle R^2 \rangle_{\text{restr}}$ for various values of G at 300K

| G (cal mol ⁻¹ Å ⁻²) | $\langle R^2 \rangle$ (Å ²) | $\langle C \rangle$ (Å) | $\langle R^2 \rangle_{\text{restr}}$ (Å ²) |
|---|--|----------------------------|---|
| 0 | 376 | — | 1064 |
| 50 | 696 | — | — |
| 100 | 800 | — | 1269 |
| 200 | 919 | — | 1270 |
| 300 | 850 | — | 1282 |
| 500 | 1066 | 2.201 | 1288 |
| 1000 | 1242 | 2.404 | 1299 |
| 2000 | 1294 | 2.469 | 1310 |
| 5000 | 1315 | 2.498 | 1313 |
| 10000 | 1327 | — | 1325 |
| ∞* | 1330 | 2.515 | 1330 |

* Limiting values of $\langle R^2 \rangle$, $\langle C \rangle$ and $\langle R^2 \rangle_{\text{restr}}$ for fully extended conformation

Table 2 The values of $\langle R^2 \rangle$, $\langle C \rangle$ and $\langle R^2 \rangle_{\text{restr}}$ for various values of G at 550K

| G (cal mol ⁻¹ Å ⁻²) | $\langle R^2 \rangle$ (Å ²) | $\langle C \rangle$ (Å) | $\langle R^2 \rangle_{\text{restr}}$ (Å ²) |
|---|--|----------------------------|---|
| 0 | 308 | — | 940 |
| 500 | 801 | 1.757 | 1246 |
| 1000 | 948 | 1.929 | 1270 |
| 2000 | 1124 | 2.259 | 1287 |
| 3000 | 1226 | 2.388 | 1295 |
| ∞* | 1330 | 2.515 | 1330 |

* Limiting values of $\langle R^2 \rangle$, $\langle C \rangle$ and $\langle R^2 \rangle_{\text{restr}}$ for fully extended conformation

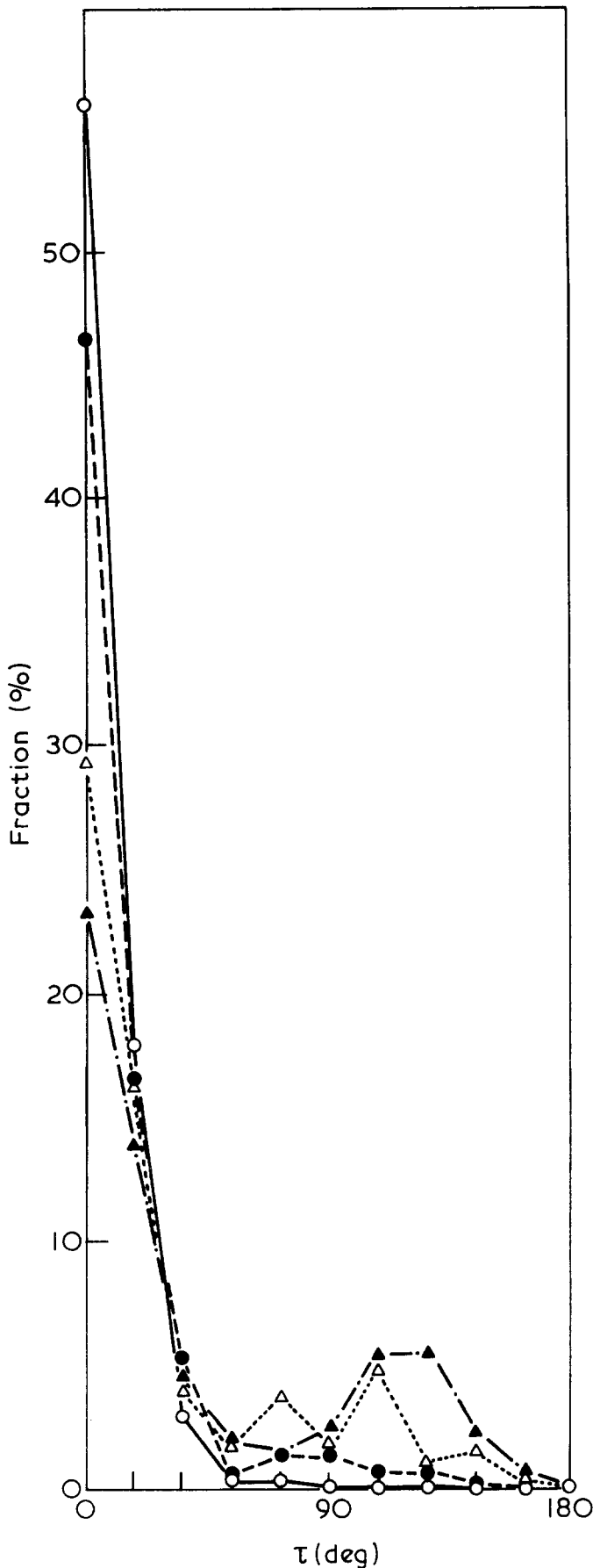


Figure 7 Normalized distributions $\rho(\tau)$ of internal rotation angles τ at 300 K for $G = 0$ (\blacktriangle), $G = 500$ (\triangle), $G = 1000$ (\bullet) and $G = 2000$ (\circ). Since $\rho(\tau)$ is a symmetric function of τ , $\rho(\tau) = \rho(-\tau)$, the distributions are plotted for positive values of τ only

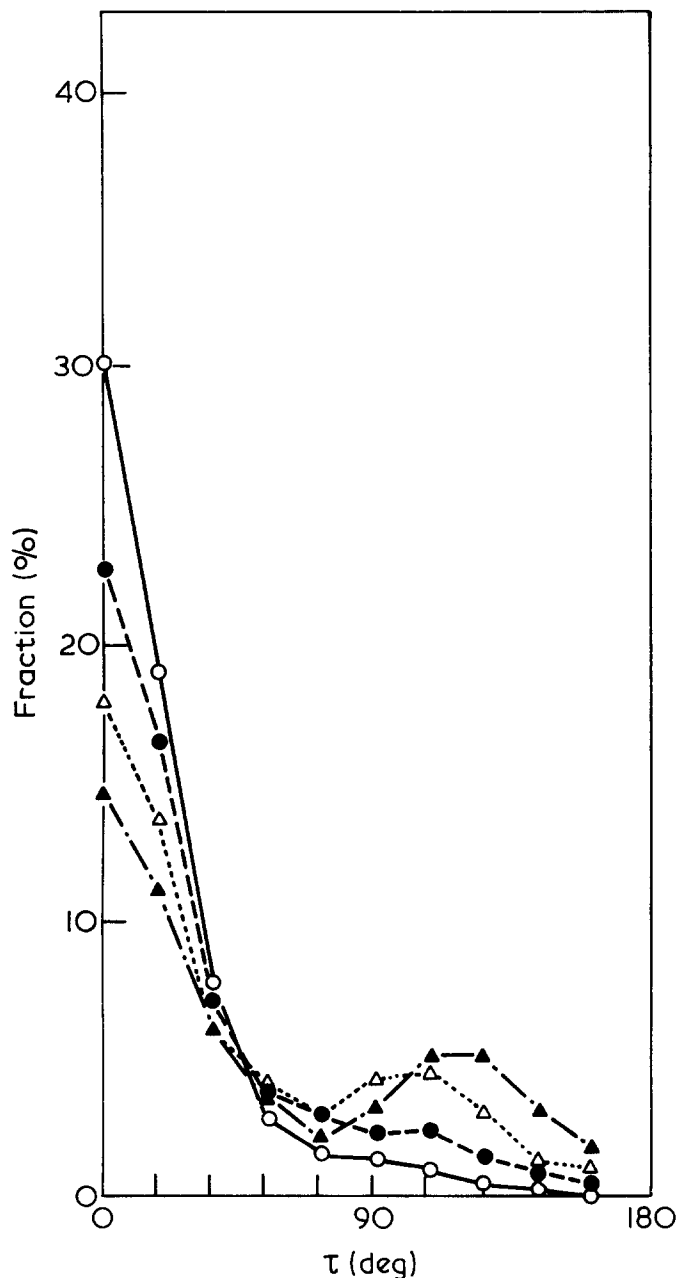


Figure 8 Normalized distributions $\rho(\tau)$ of internal rotation angles τ at 550 K for $G = 0$ (\blacktriangle), $G = 1000$ (\triangle), $G = 2000$ (\bullet) and $G = 3000$ (\circ). Since $\rho(\tau)$ is a symmetric function of τ , $\rho(\tau) = \rho(-\tau)$, the distributions are plotted for positive values of τ only

A harmonic oscillation of bonds would be completely determined by its root-mean-square deviation. When we are considering unharmonic oscillation, however, the detailed distribution of the internal rotation angles is necessary. Figure 7 shows the distribution of internal rotation angles for various values of G at 300K. For small values of G , $G=0$ for example, the distribution indicates clear peaks around *trans* and *gauche* positions. The rotational isomeric model is, therefore, a reasonable model for small values of G , especially at low temperature. With the increase of interchain potential G , the distribution around *gauche*, especially on the high-angle side of the peak, becomes suppressed, and the position of the *gauche* peak shows a remarkable shift to lower angle. At large G , the excitation of large internal rotation requires large interchain energy. This leads to the observed shift of *gauche* peak from the usual angle of 120° at $G=0$ to lower

angles at large G . In this way it is shown that a simple picture of chain conformation based on the rotational isomeric model must be discarded for a chain in the crystal. The halfwidth, $\Delta\tau$, of the peak around the *trans* state decreases with increase of G , from $\Delta\tau = \pm 23^\circ$ at $G = 0$ to $\Delta\tau = \pm 12^\circ$ at $G = 5000$. A low-frequency acoustic mode of vibration of the single chain is considered to be suppressed at large G by the increase of interchain interactions.

Figure 8 shows the distribution of the internal rotation angles at 550K. Both peaks around *trans* and *gauche* positions are significantly broadened. At $G = 0$, for example, both peaks broaden about 1.2 times those at $G = 0$ at 300K, filling the valley between the two peaks.

It is well known that polyethylene has an anomalous phase at pressures and temperatures higher than about 4 kbar and 240°C, in which the chains have a highly disordered conformation but still retain liquid-crystalline order⁵⁻⁸. The conformation of the chain in this phase was studied by X-ray diffraction on the basis of a particular model of the disordered conformation⁸. The present simulation enables us to examine the conformation in detail in this phase without recourse to any particular model of the disordered conformation. The observed contraction of the fibre period is about 5% in this phase⁸, from which the value of G can be estimated as $G = 3000 \text{ cal mol}^{-1} \text{ \AA}^{-2}$ (Table 2). The detailed distribution of angles τ in this high-pressure phase simulated in this way is, therefore, given by the graph for $G = 3000$ at 550K in Figure 8.

As seen in the graph for $G = 3000$ in Figure 8, large-amplitude oscillation around *trans* is observed: $\Delta\tau = \pm 25^\circ$. Nevertheless, the excitation of *gauche* bond is scarce and no subpeak around *gauche* is found. This is

because of the strong interchain interactions under high pressure. The effect of high pressure and high temperature on the conformation of the chain in the crystal is thus clarified: it suppresses the excitation of bonds largely deviated from *trans* and gives rise to the large-amplitude oscillations around *trans*.

CONCLUSION

By applying the Monte Carlo method to a chain in a cylindrical potential field, various behaviours of the chain were simulated. The remarkable usefulness of the method is now evident. To study the intrachain short-range order of the disordered chain, the effects of varying functional form of interchain potential $\Phi(r)$ and energy of internal rotation $E(\tau)$, etc., are the subjects of future studies.

ACKNOWLEDGEMENT

The author wishes to express his gratitude to Professor T. Hara for his encouragement throughout this work.

REFERENCES

- 1 Curro, J. G. *J. Chem. Phys.* 1974, **61**, 1203
- 2 Rosenbluth, M. N. and Rosenbluth, A. W. *J. Chem. Phys.* 1955, **23**, 359
- 3 Teramoto, E., Kurata, K., Chujo, R., Suzuki, C., Tani, K. and Kajikawa, T. *J. Phys. Soc. Jpn.* 1955, **10**, 953
- 4 Yamamoto, T. and Hara, T. *Polymer* 1982, **23**, 521
- 5 Bassett, D. C., Block, S. and Piermarini, G. *J. Appl. Phys.* 1974, **45**, 4149
- 6 Yasuniwa, M., Enoshita, R. and Takemura, T. *Jpn. J. Appl. Phys.* 1976, **15**, 1421
- 7 Yamamoto, T., Miyaji, H. and Asai, K. *Rep. Prog. Polym. Phys. Jpn.* 1976, **19**, 191
- 8 Yamamoto, T. *J. Macromol. Sci.-Phys.* 1979, **16**, 487